

A Universality in Oscillating Flows

K. L. Ekinci*, D. M. Karabacak†, and V. Yakhot
*Department of Aerospace and Mechanical Engineering,
 Boston University, Boston, Massachusetts, 02215*
 (Dated: February 6, 2020)

The law of similarity [1, 2] is the most basic consequence of the Navier-Stokes equations of fluid dynamics: two geometrically similar flows with different velocities and viscosities but equal Reynolds numbers can be made identical by rescaling the measurement units. Similarity turns into universality [3] if other features – such as the constitutive stress-strain relations, the flow geometry, and other dynamical aspects – can all be incorporated into the scaling. Here, we show that oscillating flows of simple fluids can be described in both Newtonian and non-Newtonian regimes by a universal function of a single dimensionless scaling parameter $\omega\tau$, where ω is the oscillation (angular) frequency and τ is the fluid relaxation-time; geometry and linear dimension bear no effect on the flow. Experimental energy dissipation data of mechanical resonators in a rarefied gas follow this universality closely in a broad linear dimension (10^{-6} m $< L < 10^{-2}$ m) and frequency (10^5 Hz $< \omega/2\pi < 10^8$ Hz) range. Our results suggest a deep connection between flows of simple and complex fluids [4].

In Newtonian fluid dynamics, the law of similarity establishes quantitative relations between flows of different fluids past geometrically similar objects. It is due to this law that an engineer can accurately predict flow in full-scale designs by making measurements on scaled-down models. For *steady* flows past solid bodies, for instance, the law of similarity can be formulated [2] in terms of the velocity field u :

$$u = Uf\left(\frac{r}{L}, \text{Re}\right) \quad (1)$$

Here, U is a characteristic velocity of the flow, r represents the position vector, L is a dynamically relevant linear dimension, and $\text{Re} = UL/\nu$ is the Reynolds number with kinematic viscosity ν . The dimensionless scaling function f , which reflects subtle features of the flow, is found from the Navier-Stokes equations. In unsteady flows varying on a characteristic time-scale $T = L/U$, in addition to Re , one must consider the Strouhal number, $\text{St} = \frac{L}{UT}$. Then, the similarity law of equation (1) takes the form $u = Uf\left(\frac{r}{L}, \text{Re}, \text{St}\right)$. This form is valid, for instance, when the time-dependence is induced by an *external* force varying on a time-scale T . If, however, unsteadiness is the result of *internal* flow dynamics, such as in vortex shedding behind a solid body, then St disappears from the similarity law [2]. Defining the mean free-path and relaxation time as λ and τ , respectively, one can express ν in terms of these microscopic parameters as $\nu \approx \lambda^2/\tau \approx \lambda c_s$, where c_s is speed of sound.

The equations of fluid dynamics can be formulated in the most general form as

$$\frac{\partial u_i}{\partial t} + (u \cdot \nabla)u_i = \nabla_j \sigma_{ij}, \quad (2)$$

where $i, j = x, y, z$. The stress tensor σ_{ij} can be expanded in powers of the Knudsen ($\text{Kn} = \lambda/L$) and the Weissenberg number ($\text{Wi} = \tau/T$) [5, 6, 7]: $\sigma_{ij} = \sigma_{ij}^{(1)} + \sigma_{ij}^{(2)} + \dots$. Newtonian fluid dynamics, where $\sigma_{ij} = \sigma_{ij}^{(1)} = \frac{\mu}{2} \left(\frac{\partial u_i}{\partial x_j} + \frac{\partial u_j}{\partial x_i} \right)$ with $\mu = \rho\nu$, corresponds to the first term of the expansion. To show this, simply consider flow past a bluff body of linear dimension L : with velocity gradient $\sim \frac{U}{L}$, $\frac{\sigma}{\rho U^2} \approx \frac{\lambda c_s}{L U} \approx \frac{\text{Kn}}{\text{Ma}}$; here, $\text{Ma} = U/c_s$ is the Mach number. The Newtonian approximation is thus valid only when $\text{Kn} \ll 1$. Given that $\lambda \approx c_s \tau$, it is easy to see that $\text{Kn} = \frac{\lambda}{L} \approx \frac{c_s \tau}{L U} \approx \frac{\text{Wi}}{\text{Ma}}$ and $\frac{\sigma}{\rho U^2} \approx \frac{\text{Wi}}{\text{Ma}^2}$. Consequently, for fixed Ma , $\text{Kn} \ll 1$ and $\text{Wi} \ll 1$ correspond to the same physical limit: the Newtonian flow regime. This statement is also accurate in unsteady flows past a bluff body, where the shed vortices may be thought to introduce independent time (Wi) and length scales (Kn). Yet, the characteristic oscillation frequency for vortex shedding is $\Omega = \frac{2\pi U \text{St}}{L}$, where $0.1 \leq \text{St} \leq 1$ over a wide range of Re depending on geometry. Thus, $\Omega\tau = \frac{2\pi\tau}{T} \sim \frac{\lambda U}{L c_s}$, and Wi and Kn are linked. It is then straightforward to conclude that Newtonian fluid dynamics, and consequently, the similarity relation in equation (1), should be valid for *slowly varying large-scale* flows: $\text{Kn} \ll 1$ and $\text{Wi} \ll 1$.

Recent advances in micro- [8] and nanotechnology [9], biofluid mechanics [10], rheology [4], and so on have resulted in flows at unusual time scales ($\text{Wi} \geq 1$) and length scales ($\text{Kn} \geq 1$), where the Newtonian approximation breaks down. Many interesting phenomena, such as elastic turbulence [11], structural relaxation of soft matter [12] and enhanced heat transfer in the nanoparticle-seeded fluids [13], have been observed in this range of parameters. Thus, the basic theoretical question of possibility of a universal description covering both Newtonian and non-Newtonian flow regimes is of great importance and interest for both fundamental physics and engineering.

For a similarity law valid in both Newtonian and non-

*Corresponding author: ekinci@bu.edu

†Current address: Holst Centre/IMEC-NL, High Tech Campus 31, PO Box 8550, 5605 KN Eindhoven, The Netherlands.

Newtonian limits, the scaling relation in equation (1) must be modified as

$$u = Uf\left(\frac{r}{L}, \frac{r}{\delta}, \frac{\lambda}{L}, \frac{\lambda}{\delta}, \frac{\tau}{T}, \text{Re}, \text{St}\right). \quad (3)$$

Here, in addition to the above parameters, a dynamic length scale δ to be clarified below, may enter the scaling function f . To assess the relative importance of various dimensionless parameters, we investigate the second order correction to the stress tensor derived from the Boltzmann equation [5, 6, 7]:

$$\sigma_{ij}^{(2)} \approx \rho\lambda^2 \frac{\partial u_i}{\partial x_\alpha} \frac{\partial u_j}{\partial x_\alpha} \quad (4)$$

Considering first the shed vortices behind a body, we readily estimate the second order correction to the stress tensor from equation (4) as $\sigma^{(2)} \approx \rho\lambda^2 U^2/L^2$. Thus, $\sigma^{(1)} + \sigma^{(2)} \approx \rho\nu\frac{U}{L} + \rho\lambda^2\frac{U^2}{L^2} \approx \rho\nu\frac{U}{L}\left(1 + \frac{U}{c_s}\frac{\lambda}{L}\right) \approx \rho\nu\frac{U}{L}\left(1 + \frac{\tau}{T}\right)$. In this simple case, σ appears as an expansion in powers of Kn or, equivalently, in powers of Wi.

In another classic problem – laminar steady flow over a semi-infinite flat plate illustrated in Fig. 1a – the relationship between Kn and Wi can still be stated, albeit with important differences from above. The key dynamic feature of this flow is the viscosity-dominated boundary layer of thickness $\delta = \sqrt{\frac{x\nu}{U}}$ (see coordinate axis in Fig. 1a). Here, U is the free-stream velocity outside the boundary layer. The Newtonian approximation results in a stress field $\sigma_{xy}^{(1)} = \rho\nu\frac{\partial u_x}{\partial y} \approx \rho c_s\lambda\frac{U}{\delta}$. With the symmetries in the problem, the contributions to the stress tensor of the kind given in equation (4) disappear, resulting in a second order correction [5], $\sigma_{xy}^{(2)} = \rho\lambda^2\frac{\partial u_x}{\partial y}(\nabla \cdot u) \approx \rho\lambda^2\frac{U^2}{x\delta}$. Thus, the expansion becomes $\sigma_{xy}^{(1)} + \sigma_{xy}^{(2)} \approx \rho c_s\lambda\frac{U}{\delta}\left(1 + \frac{\lambda U}{xc_s}\right) \approx \rho c_s\lambda\frac{U}{\delta}\left(1 + \frac{\lambda^2}{\delta^2}\right)$, with the second-order correction of order $(\frac{\lambda}{\delta})^3$. Note that the second order term can also be expressed as Wi since $x/U = T$. This example establishes that the relevant linear dimension δ is no longer a geometric dimension of the body but a dynamic characteristic of the flow and $\text{Kn}_\delta \equiv \lambda/\delta \propto \sqrt{\text{Wi}}$ emerges as the scaling parameter.

Even more unexpected conclusions emerge for the *unsteady* flow generated by an infinite plate oscillating at (angular) frequency ω with peak velocity and amplitude U and A , respectively (Fig. 1b and c) [14]. In the Newtonian limit $\omega\tau \ll 1$, the Stokes boundary layer thickness, $\delta = \sqrt{\frac{2\nu}{\omega}}$, is the only length scale in the problem. In this limit, $\text{Kn}_\delta \propto \sqrt{\text{Wi}}$ holds as above, since $\text{Kn}_\delta = \frac{\lambda}{\delta} \approx \sqrt{\frac{\omega\lambda^2}{\nu}} \approx \sqrt{\omega\tau}$. Due to its geometric simplicity, this problem can be solved in the entire dimensionless frequency range, $0 < \omega\tau < \infty$ by a summation of the Chapman-Enskog expansion of kinetic theory [15, 16] and non-perturbatively [17]. The analytic solution for the velocity field is obtained as

$$u_x(y) = Ue^{-y/\delta_-} \cos(\omega t - y/\delta_+), \quad (5)$$

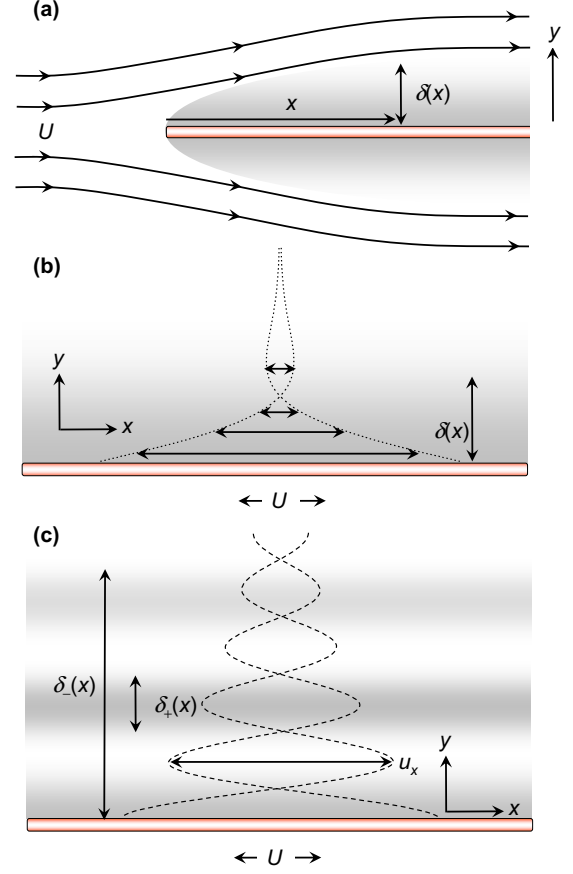


FIG. 1: (color online). Flow geometries and dynamical parameters. (a) Laminar steady flow over a semi-infinite flat plate. A viscous boundary layer of thickness $\delta(x)$ is formed on the plate. The characteristic velocity is the free stream velocity U outside the boundary layer. (b) Unsteady flow and viscous boundary layer of thickness δ generated by an infinite oscillating plate in the Newtonian limit ($\omega\tau \ll 1$). The plate oscillates at (angular) frequency ω with peak velocity U and amplitude A , respectively. (c) The same problem in the non-Newtonian limit ($\omega\tau \geq 1$). Two new length scales, a wavelength δ_+ and a penetration depth δ_- emerge instead of the viscous boundary layer thickness δ .

with two new length scales, a wavelength δ_+ and a penetration depth δ_- :

$$\frac{\delta}{\delta_{\pm}} = (1 + \omega^2\tau^2)^{1/4} \left[\cos\left(\frac{\tan^{-1}\omega\tau}{2}\right) \pm \sin\left(\frac{\tan^{-1}\omega\tau}{2}\right) \right]. \quad (6)$$

In the limit $\omega\tau \gg 1$, δ disappears from the problem and the relevant length scale becomes the penetration depth δ_- . However, as $\omega\tau \rightarrow \infty$, the *first* Knudsen number saturates: $\text{Kn}_{\delta_-} \equiv \frac{\lambda}{\delta_-} \rightarrow \frac{1}{2}$, indicating that in this limit Kn_{δ_-} cannot appear as an expansion parameter in the

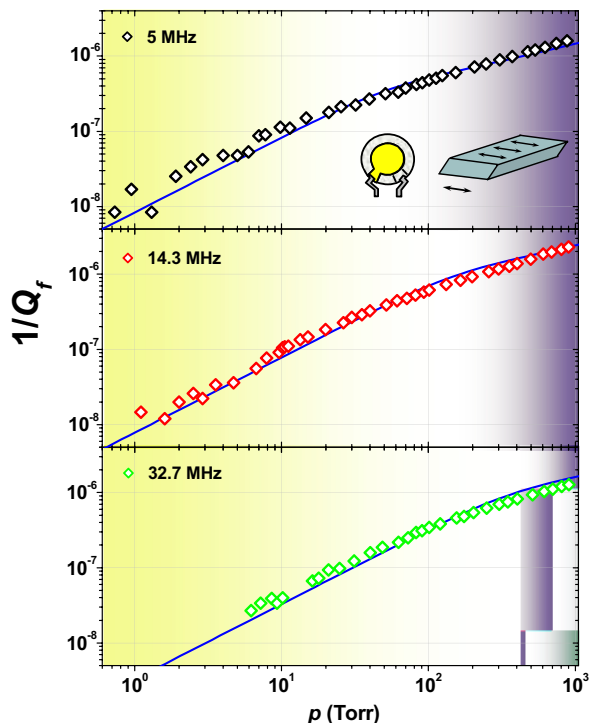


FIG. 2: (color online). Fluidic dissipation in quartz crystal resonators. Three different measurements of Q_f^{-1} at 5 MHz, 14.3 MHz and 32.7 MHz (top to bottom) are shown as a function of pressure. The inset shows an illustration of the quartz and the shear mode oscillation. Each plot shows a transition from non-Newtonian (blue) to Newtonian (yellow) flow marked by a change in slope from $Q_f^{-1} \propto p$ to $Q_f^{-1} \propto p^{1/2}$. The fits in the figure are to equation (9) using fitting factors of 0.8, 0.6 and 0.9 and $S/m = 2.754 \text{ m}^2/\text{kg}$, $9.827 \text{ m}^2/\text{kg}$ and $6.296 \text{ m}^2/\text{kg}$ (top to bottom).

stress-strain relation or as a scaling parameter in equation (3). It follows from equation (6) that the *second* Knudsen number, $\text{Kn}_{\delta_+} \equiv \frac{\lambda}{\delta_+} \rightarrow \omega\tau$, which is exactly the expansion parameter derived from the Chapman-Enskog expansion applied to the Boltzmann-BGK equation [15]. We conclude that the only relevant scaling parameter for the oscillating plate problem valid in both Newtonian and non-Newtonian regimes is

$$\text{Wi} = \omega\tau = \text{Ma} \frac{\lambda}{A}, \quad (7)$$

since $U = A\omega$. We re-emphasize that Wi does not contain any information about the linear dimensions of the oscillating body but only depends upon its oscillation amplitude A as inferred from equation (7). As long as $A \ll L$ and $\text{Re} \sim 0$, the flow over the oscillating body remains tangential along the surface, along the natural curvatures.

We provide direct experimental support for the predicted universality by studying the interaction of oscillating solid surfaces of vastly different sizes with nitrogen

gas. Nitrogen approximates an ideal gas, where τ can be effectively tuned by changing the pressure p : $\tau \propto 1/p$. For the large plate (Fig. 1c), the shear stress leads to average dissipated energy per unit time (with units of W/m^2) as $\dot{E} = \frac{SU^2}{2} f(\omega\tau) \sqrt{\frac{1}{2}\omega\mu\rho}$. Here, S is the surface area and the scaling function $f(\omega\tau)$ is [16]

$$f(\omega\tau) = \frac{1}{(1 + \omega^2\tau^2)^{3/4}} \left[(1 + \omega\tau) \cos\left(\frac{\tan^{-1}\omega\tau}{2}\right) - (1 - \omega\tau) \sin\left(\frac{\tan^{-1}\omega\tau}{2}\right) \right]. \quad (8)$$

We used mechanical resonators of different sizes: macroscopic quartz crystals, microcantilevers and nanomechanical beam resonators. We excited the resonators at very small oscillation amplitudes ($A \ll L$) around their resonances and measured their quality factors (Q) as a function of p , treating the relevant mode of the resonator as a one-dimensional damped harmonic oscillator. At a given p , the energy losses arising from the fluid and the resonator (coupled to the measurement circuit) determine the overall (loaded) quality factor as $Q_l^{-1} = [Q_f(p)]^{-1} + Q_r^{-1}$, but as the p is reduced the fluidic dissipation becomes negligible and $Q_l^{-1} \approx Q_r^{-1}$ (supplementary materials). Returning to the expression for \dot{E} above, we can write

$$Q_f^{-1} = \frac{\dot{E}}{\omega E_{st}} = \frac{S}{m} f(\omega\tau) \sqrt{\frac{\mu\rho}{2\omega}}, \quad (9)$$

where $E_{st} = \frac{mU^2}{2}$ is the energy stored in the mechanical resonator. Q_f^{-1} depends upon p through τ and ρ , and follows two different asymptotes $Q_f^{-1} \propto p$ (non-Newtonian) and $Q_f^{-1} \propto p^{1/2}$ (Newtonian) at high p and low p , respectively. The transition between the asymptotes takes place at $\omega\tau \approx 1$, and shifts to higher p as ω is increased since $\tau \propto 1/p$.

We first show the basic aspects of the universality on similar sized macroscopic quartz crystal resonators with different resonance frequencies. Fig. 2 shows Q_f^{-1} for quartz resonators moving in fundamental shear mode (inset) as a function of p at $\omega/2\pi = 5, 14.3$ and 32.7 MHz (top to bottom). Q_f^{-1} was obtained by properly accounting for resonator losses (see supplementary materials). The transition from non-Newtonian (blue) to Newtonian (yellow) flow regime is apparent in each plot as a change in slope. The transition pressure from multiple resonators with different frequencies can be used to extract the proportionality constant as [16] $\tau \approx \frac{1.85 \times 10^{-6}}{p}$ (τ is in s when p is in Torr) (supplementary materials). The fits in the figure are obtained using the expression in equation (9) with experimentally measured S/m values (supplementary materials), standard μ and ρ values, and the empirical relation between τ and p . The flow for the small amplitude shear mode oscillations matches

the large plate problem to a very good approximation [18, 19]. The only non-ideality comes from the velocity distribution on the surface of the resonator [20], which may be the reason for the small deviation of the fitting factors from unity.

The universality requires that the characteristics of the flow remain size and shape independent. Our energy dissipation measurements from resonators spanning a broad range of linear dimension L and oscillating in different modes establish this aspect. Fig. 3a shows energy dissipation measurements on three different devices as a function of p (x-axis) and L (y-axis): a macroscopic quartz resonator in shear-mode at 14.3 MHz, a microcantilever and a nanomechanical beam resonator in flexural modes at 1.97 MHz and 23 MHz, respectively. Note that Q_f^{-1} (z-axis) is normalized [16] by S/m , since the stored energy is proportional to m , while the dissipated energy is proportional to S . For the dynamically relevant linear dimension of the flow, we use $L \approx \sqrt{S}$ determined by the surface area. For the quartz crystal, $L_Q \approx 10^{-2}$ m, set roughly by the electrode diameter [21, 22]. For the cantilever, $L_C \approx 10^{-4}$ m and for the doubly-clamped-beam, $L_C \approx 5 \times 10^{-6}$ m. The flow is illustrated in the upper inset for flexural modes; as noted above, it follows the gentle curvatures tangentially as long as $A \ll L$. In the pressure range studied, the traditional Kn ($\text{Kn} = \lambda/L$) span roughly the range between $10^{-6} < \text{Kn}_Q < 10^{-2}$, $10^{-4} < \text{Kn}_C < 1$, and $10^{-2} < \text{Kn}_B < 10^2$. Two things are noteworthy: all curves look similar, and L or Kn appears to have no effect on the flow. The dimensionless scaling functions $f(\omega\tau)$ of equation (9) extracted from each resonator in this study is shown as a function of $\omega\tau$ in Fig. 3(b) with the theoretical prediction. The rationale for using slightly larger fitting factors of 2.8 for the out-of-plane modes is explained in supplementary materials.

In our experiments, τ is determined by the microscopic interaction of gas molecules and a solid surface. By naively treating the nitrogen as a gas of hard spheres, one can obtain $\tau \approx \frac{0.180 \times 10^{-6}}{p}$ (τ is in s when p is in Torr). This value, however, only reflects interactions between gas molecules, as would happen away from surfaces in the bulk region of the gas. The observed dependence, which is roughly an order of magnitude larger, points to the importance of gas-surface interactions.

Here, we considered oscillating flows of simple geometries with $\text{Re} \sim 0$, where non-linear effects, like hydrodynamics instabilities and viscoelastic turbulence are not present. Our experimental data provide evidence for a transition in oscillating flows of simple gases from purely viscous (Newtonian) to viscoelastic (non-Newtonian) dynamics. This transition is due to the *intrinsic* dynamic response of the simple fluid to high-frequency perturbations. Similar observations are commonplace in macroscopic flows of concentrated long-chain polymer solu-

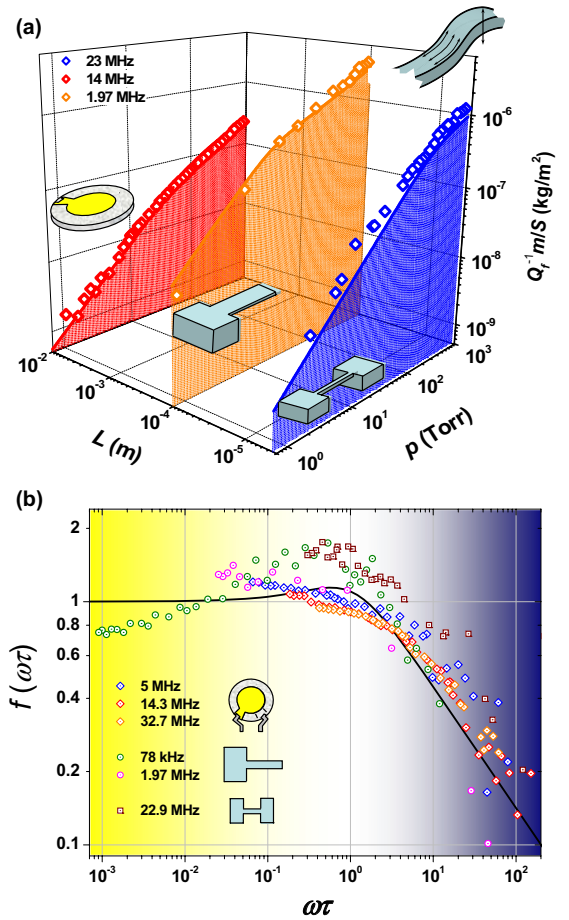


FIG. 3: (color online). Fluidic dissipation across length scales. (a) Typical dissipation measurements for a macroscopic quartz resonator, a microcantilever and a nanomechanical doubly-clamped beam resonator as a function of pressure (x-axis) and characteristic linear dimension (y-axis). The resonators are illustrated in the inset. The quartz crystal has a diameter of 1 cm with an electrode (yellow) diameter roughly half of this on both sides; its thickness is ~ 0.1 mm. It moves in its *fundamental shear mode* at $\omega/2\pi = 14.3$ MHz. The microcantilever has dimensions $125 \mu\text{m} \times 36 \mu\text{m} \times 3.6 \mu\text{m}$ (length \times width \times thickness) and moves in its first flexural harmonic mode in the out-of-plane direction at $\omega/2\pi = 1.97$ MHz. The nanomechanical beam has dimensions $17 \mu\text{m} \times 500 \text{nm} \times 280 \text{nm}$ (length \times width \times thickness) and moves in its *fundamental flexural mode* in the out-of-plane direction at $\omega/2\pi = 22.9$ MHz. Q_f^{-1} from different devices were normalized by S/m , since the stored energy is proportional to resonator mass m , while the dissipated energy is proportional to surface area S . The relevant linear dimension for each resonator was obtained from its surface area as $L \approx \sqrt{S}$. The flow on the surfaces during flexural oscillations is illustrated in the upper inset. The transition at $\omega\tau \approx 1$ takes place at $p = 17.5, 40,$ and 216 Torr for the 1.97, 14.3 and 22.9 MHz resonators, respectively. The solid lines are obtained from equation (9) using fitting factors 0.6 for the quartz resonator, and 2.8 for the cantilever and the beam. (b) The scaling function $f(\omega\tau)$ extracted for each resonator. Data at 78 kHz from the fundamental out-of-plane flexural mode of the above micro-cantilever is added to all the data of Fig. 2 and Fig. 3(a). The S/m values for the micro and nanodevice are as follows: $S/m = 688 \text{ m}^2/\text{kg}$ (78 kHz cantilever), $S/m = 405 \text{ m}^2/\text{kg}$ (1.97 MHz Cantilever), $S/m = 4013 \text{ m}^2/\text{kg}$ (22.9 MHz beam).

tions, where τ can be long and, consequently, $Wi \geq 1$ due to the relatively slow polymer dynamics [4, 11, 23]. In rheology, the polymers are often treated as elastic springs, and viscoelastic behavior of polymer solutions is attributed to the direct polymer contribution to the stress tensor. Thus, our work demonstrates a deep dynamical connection of the oscillating flows of complex and simple fluids.

We thank N. O. Azak and M. Y. Shagam for experimental help and A. Vandelay for useful discussions. This work was supported by Boston University through a Dean's Catalyst Award and by the National Science Foundation through the Division of Chemical, Bioengineering, Environmental, and Transport Systems (Fluid Dynamics Programme).

-
- [1] O. Reynolds, *Phil. Trans. Roy. Soc.* **174**, 935 (1883).
 [2] L. D. Landau and E. M. Lifshitz, *Fluid Mechanics* (Pergamon Press, Oxford, 1959).
 [3] H. Tanaka, *Phys. Rev. Lett.* **76**, 787 (2006).
 [4] R. B. Bird, R. C. Armstrong, and O. Hassager, *Dynamics of polymeric liquids, Vol. 1 Fluid Mechanics*, R. B. Bird, C. F. Curtis, R. C. Armstrong, and O. Hassager, *Dynamics of polymeric liquids, Vol. 2 Kinetic Theory* (John Wiley, New York, 1987).
 [5] L. D. Landau and E. M. Lifshitz, *Physical Kinetics* (Butterworth-Heinemann, Oxford, 1981).
 [6] H. Chen, S. A. Orszag, I. Staroselsky, and S. Succi, *J. Fluid Mechanics* **519**, 301 (2004).
 [7] C. Cercignani, *Theory and application of the Boltzmann equation* (Elsevier, New York, 1975).
 [8] T. Squires and S. R. Quake, *Rev. Mod. Phys.* **77**, 977 (2005).
 [9] K. L. Ekinici and M. L. Roukes, *Rev. of Sci. Instr.* **76**, 061101 (2005).
 [10] A. D. Stroock, S. K. W. Dertinger, A. Ajdari, I. Mezic, H. A. Stone, and G. M. Whitesides, *Science* **295**, 647 (2002).
 [11] A. Groisman and V. Steinberg, *Nature* **405**, 53 (2000).
 [12] H. M. Wyss, K. Miyazaki, J. Mattsson, Z. Hu, D. R. Reichman, and D. A. Weitz, *Phys. Rev. Lett.* **98**, 238303 (2007).
 [13] X. Wang, X. Xu, and S. U. S. Choi, *J. of Thermophysics and Heat Transfer* **13**, 474 (1999).
 [14] P. J. Petersan and S. M. Anlage, *Trans. Cambridge Philos. Soc.* **9**, 8 (1851).
 [15] V. Yakhot and C. Colosqui, *J. Fluid Mechanics* **586**, 249 (2007).
 [16] D. M. Karabacak, V. Yakhot, and K. L. Ekinici, *Phys. Rev. Lett.* **98**, 254505 (2007).
 [17] H. Chen, S. A. Orszag, and I. Staroselsky, *J. Fluid Mechanics* **574**, 495 (2007).
 [18] C. D. Stockbridge, *Vacuum Microbalance Techniques*, vol. 5 (Plenum, New York, 1966).
 [19] J. Krim and A. Widom, *Phys. Rev. B* **38**, 12184 (1988).
 [20] B. A. Martin and H. E. Hager, *J. Appl. Phys.* **65**, 2630 (1989).
 [21] M. Herrscher, C. Ziegler, and D. Johannsmann, *J. Appl. Phys.* **101**, 114909 (2007).
 [22] B. Capelle, J. Detaint, A. Zarka, Y. Zheng, and J. Schwartzel, *Proceedings of the 44th Annual Symposium on Frequency Control* pp. 416–423 (1990).
 [23] J. J. Magda and R. G. Larson, *J. Non-Newtonian Fluid Mech.* **30**, 1 (1988).